11th World Congress on Computational Mechanics (WCCM XI)
5th European Conference on Computational Mechanics (ECCM V)
6th European Conference on Computational Fluid Dynamics (ECFD VI)
E. Oñate, J. Oliver and A. Huerta (Eds)

COMPUTATIONAL AND EXPERIMENTAL MODEL OF NANO-ENGINEERED DRUG DELIVERY SYSTEM FOR TRABECULAR BONE

HOSSEIN MOKHTARZADEH[*], MOOM S. AW[†], KAMARUL A. KHALID[Φ§], KARAN GULATI[†], GERALD J. ATKINS[Φ], DAVID M. FINDLAY[Φ], AND DUSAN LOSIC[†], PETER PIVONKA[*]

[*]Australian Institute of Musculoskeletal Science, Northwest Academic Centre, University of Melbourne, Australia, mhossein@unimelb.edu.au
[†]School of Chemical Engineering, University of Adelaide, Adelaide, SA 5005, Australia
[Φ]Discipline of Orthopaedics and Trauma, University of Adelaide, Adelaide, SA 5005, Australia
[§]Department of Orthopaedics, Traumatology & Rehabilitation, Faculty of Medicine, International Islamic University Malaysia, Kuantan, Pahang 25200, Malaysia

Key Words: *Advection-diffusion equation, Local drug delivery, Bioreactor, Bone, Porous media*

Abstract. This paper describes fully coupled advective-diffusive transport of a drug through a trabecular bone sample in a perfused bioreactor. We used the analogy between heat transfer and mass transfer in order to derive the effective transport properties of the porous material such as effective diffusion coefficient and permeability. This allowed employing the heat transfer equations in Abaqus and they were solved using the finite element (FE) method. The average velocity was calculated using the *Darcy-Brinkman-Forchheimer* equation. Simulation results suggest that effective diffusivity plays a major role in the spatio-temporal distribution of the drug in the bone sample. Bone permeability was found less effective on manipulating the spatial distribution of drug. The bioreactor perfusion rate played a major role in the distribution of the drug throughout the bone sample. Increased perfusion rate leads to clearance of the drug towards the outlet of the bioreactor. It was found that even for moderate bioreactor perfusion rates the drug was concentrated towards the outlet, while zero concentration of drug was observed around the inlet. The numerical simulations showed that the essential effects of local drug release in bone can be captured using fluid flow through porous media theory. Our simulation results revealed that drug delivery is a multi-factorial phenomenon. Therefore, a mathematical model can enhance our understanding of this complicated problem that is difficult to characterize using experimental techniques alone.

1 INTRODUCTION

Bone diseases, as a major health issue, cost both individual patients and society to be treated. To treat bone diseases, systemic drug administration can be utilized. However, the conventional systemic drug deliveries are accompanied with several limitations including lack of high efficacy, bioavailability and biodistribution in addition to other side effects on non-

target tissues including drug overdose and toxicity [1]. Local drug delivery using drug-releasing implants located inside bone is recognized as a promising strategy to address the limitations of systemic drug administration to bone. However, the studies of optimum drug-release kinetics are not possible to perform using existing in-vitro drug releasing systems and 2-D bone cell models without several trial and errors.

Bone is a porous material consisting of a solid and a fluid phase. Local drug delivery in bone is dependent on the perfusion rate of the drug (i.e., advective transport) and the concentration gradient of drug (i.e., diffusive transport). Explanation of the bioreactor set up experimental methods have shown drug kinetics using nanotubes porous medium allows certain level of perfusion, however, it is somehow impractical to optimize drug delivery system with a number of aforementioned parameters, in an experimental setup. Several mathematical models have been developed to address drug release kinetic; however, the role of biochemical and biomechanical variables on drug release kinetics in a bioreactor has not been fully understood [1-3]. Mathematical models enable us to predict and optimize drug release kinetics in *in-silico* simulations using porous media theories.

The aim of this work is to demonstrate the use of a 3-D bone bioreactor for studying the drug-release kinetics and distribution of drugs in the ex-vivo trabecular bone environment using finite element methods in Abaqus. A fully coupled fluid flow in a porous media with diffusion has been used to study the role of different design variables on drug distribution in a bioreactor. The role of the following variables on drug distribution was investigated in this study: permeability, perfusion rate, porosity, and effective diffusivity. The results of our simulations can be used for validation of 3D bioreactors and prediction of drug release and distribution under different design conditions. Therefore, we ultimately aim to develop a mathematical model to predict the combined role of aforementioned variables on the effectiveness of 3D bioreactor to design tissue engineered materials and to optimize local drug delivery systems.

2 METHODS

In order to simulate local drug transport in the trabecular bone bioreactor, the classic advection-diffusion equation for porous materials can be applied. In the following we will use the analogy between the heat and diffusion problem to address local drug delivery in a porous medium, i.e., trabecular bone sample. The mathematical analogy between the heat transfer equation and mass transfer equations was adopted to simulate drug release in a porous material [2]. For pure fluids the energy conservation equation reads:

$$\rho c \frac{\partial T}{\partial t} = -\nabla \cdot \mathbf{J}_H + \mathrm{Q} \tag{1}$$

Where ρ is the fluid density, c is the specific heat capacity, T is fluid temperature, and Q is a heat source/sink term. The heat flux can be defined as:

$$\mathbf{J}_H = -k \ \ \nabla T + \boldsymbol{v} T \tag{2}$$

Where k is heat thermal conductivity and $\boldsymbol{v}$ is the prescribed convective velocity of the fluid.

On the other hand, the mass balance equation can be written as:

$$\frac{\partial c}{\partial t} = -\nabla \cdot \mathbf{J}_c + \dot{\mathrm{S}} \tag{3}$$

Where c is the concentration of solute, and S is a mass source/sink term. The flux transport of solute can be expressed as:

$$\mathbf{J}_c = -D \ \ \nabla \mathrm{c} + \boldsymbol{v}c \tag{4}$$

Where D is the solute diffusion coefficient and $\boldsymbol{v}$ the prescribed advective velocity of the fluid. In Eqn.(4) the first term on RHS represents Fick's first law describing pure diffusion driven by a gradient in concentration, while the second term is forced advection due to fluid motion. Comparing the individual coefficients in Eqn. (1), (2) and Eqn. (3), (4) an analogy between heat and mass transfer can be identified. The corresponding variables in these equations are summarized in Table 1.

In the Section 2.2 we will give a similar analogy for heat and mass transfer through porous materials.

Table 1: Comparison of heat and mass transfer parameters adopted from [2]

Heat transfer		***Mass transfer***	
Symbol	Description	Symbol	Description
T	Temperature	C	Concentration
ρ	Density	ρ	Density
K	Thermal conductivity	k	mass diffusion coefficient
c	Specific heat capacity	1/ ρ	(ρ times c) =1
v	Fluid velocity	v	Convection velocity
$\dot{\mathrm{Q}}$	Heat generation rate per unit volume	$\dot{\mathrm{S}}$	Drug generation rate per unit volume

2.1 Isothermal fluid flow in porous media

In the following we assume that the fluid flow through the bone sample is incompressible (Eqn. (5)). In order to address the problem of fluid flow through the bone sample in the bioreactor we apply the Darcy-Brinkman- Forchheimer equation [4]. This equation is based on volume averaging of the Navier-Stokes equation applied to the fluid phase of the porous material [4]. This equation takes into account interactions of the fluid with the solid phase and also inertial effects. In case the latter effects can be neglected the classical Darcy law for fluid flow through a porous material is obtained. This equation is derived assuming that the porosity of the material is constant and that the permeability is isotropic:

$$\nabla . v = 0, \tag{5}$$

$$\frac{\rho}{\epsilon}\left[\frac{\partial v}{\partial t} + \boldsymbol{v}.\nabla\left(\frac{v}{\epsilon}\right)\right] = \nabla . p + \frac{\mu}{\epsilon}\,\nabla.\nabla v + \frac{\mu}{K}v - \frac{\rho C_F}{K^{1/2}}|v|v\ (1) \tag{6}$$

$\boldsymbol{v}$ is the extrinsic average velocity vector (or Darcy velocity for pure Darcy flow regime), which is the average of both solid and fluid phase, p is the intrinsic average pressure (acting in the fluid phase), ρ is the fluid density, μ is fluid viscosity, ϵ and K are the porosity and permeability of the porous medium, respectively.

In Eqn. (6) on the right hand side, the second, third and fourth terms are the Brinkman term (which considers the presence of solid boundaries), the Darcy drag term, and the Forchheimer drag term represented by C_F (which considers inertial effects proportional to the square of velocity), respectively. Given that the fluid velocities in the bioreactor are relatively small the last term can be neglected, i.e., C_F=0. Note that the velocity in the fluid phase can be estimated as $\boldsymbol{v}^f=\boldsymbol{v}/\epsilon$.

2.2 Advective-diffusive transport of drug in trabecular bone

As already outlined at the beginning of this section we will make use of the mathematical analogy between heat and diffusive transport. The conservation of energy equation for non-isothermal flows can be written as [4,5]:

$$(\rho C_P)_{eff}\frac{\partial T}{\partial t} + (\rho C_P)_{eff}\boldsymbol{v}.\nabla T = \nabla.\left(k_{eff}\nabla T\right) + q'''_{eff} \tag{7}$$

$$(\rho C_P)_{eff} = (1-\epsilon)(\rho_s C_{Ps}) + \epsilon\left(\rho_f C_{Pf}\right) \tag{8}$$

$$k_{eff} = (1-\epsilon)k_s + \epsilon k_f \tag{9}$$

Whereby, $(\rho C_P)_{eff}$ specifies the constant pressure specific heat, while k_{eff} is the effective thermal conductivity of the porous material. Note that $(\rho C_P)_{eff}$ and k_{eff} are volume averages of the fluid and solid phase of the porous material respectively (Eqn. (6) and (7)). q'''_{eff} represents a source/sink term and is the external heat supplied/extracted per unit volume. Note that this equation was derived assuming an isotropic material, negligible viscous dissipation, local thermal equilibrium and negligible heat transfer between the phases present in the porous medium. The second term on the left side of Eqn.(7) represents *thermal convective flow*, while the first term on the right side of Eqn.(7) represents *conductive flow* driven by gradients in temperature. Due to the coupling of Eqn. (6) and (7) the extrinsic average velocity vector **v** in Eqn.(7) is fully defined. Note that Eqn. (6) and (7) are semi coupled due to the fact that only Eqn.(6) influences Eqn.(7), but not vice versa.

The diffusive pendant to the energy transport equation is the conservation of mass equation:

$$\epsilon\frac{\partial C}{\partial t} + \boldsymbol{v}.\nabla C \quad = \nabla.\left(D_{eff}\nabla T\right) + S'''_{eff} \tag{10}$$

Where ϵ represents the porosity and D_{eff} is the effective diffusion coefficient. S'''_{eff} represents a volumetric concentration source/sink term respectively. Note that the second term on the left side represents *advective flow* of the solute, while the first term on the right represents *diffusive flow* driven by gradients in concentration. D_{eff} is the volume average of the

solute diffusion coefficient in the fluid phase and can generally be represented as a function of the porosity. Dividing Eqn. (7) by $(\rho C_P)_{eff}$ we obtain the following form of the conservation of energy equation:

$$\epsilon \frac{\partial T}{\partial t} + \boldsymbol{v}.\nabla T = \nabla.\left(k_{eff}\nabla T/\rho_f C_{Pf}\right) + q'''_{eff} \tag{11}$$

Since mass transfer only occurs in the fluid phase we also assume that the corresponding heat transfer takes place only in the fluid phase of the material, hence, we set parameters in the solid phase to zero:

$$C_{Ps} = k_s = 0 \tag{12}$$

Hence the effective specific heat capacity of the porous material can be expressed as:

$$(\rho C_P)_{eff} = \epsilon\left(\rho_f C_{Pf}\right) \tag{13}$$

Using the same analogy between temperature (T) and concentration (c) one obtains:

$$D_{eff} = k_{eff}/\rho_f C_{Pf} \tag{14}$$

2.3 Simulation of fully coupled advection-diffusion problem

We are using the *Zetos* 3D bioreactor for assessment of local drug delivery in trabecular bone. This bioreactor allows adjustment of the perfusion rate together with mechanical loading of the bone specimen. In the following we will assume that there is no mechanical loading of the bone specimen. Therefore, the only boundary condition characterizing the bioreactor is the perfusion rate which can be applied via pore pressure boundary conditions at the inlet and outlet. The advective-diffusion equations are solved in Abaqus 6.13-1 using the finite element (FE) method.

Bovine trabecular bone samples with cylindrical geometry have been used in previous experiments for drug delivery studies in a bioreactor [6]. The bone marrow has been cleared from these samples before experiments providing a larger pore space for fluid transport. Nano-engineered Ti wires were inserted into the bone samples using a drill with prescribed calibre. These Ti wires contained a layer of TNT arrays which can be loaded with a design drug and modified to be released at a certain rate. Aw et al. described the details of the experiments in a previous study [6].

As described in the introduction, the aim of our study is to better characterise the design variables of the bioreactor (i.e., the perfusion rate) and the influence of the variability of bone samples (i.e., permeability and diffusivity). For the current study, we do not consider the rate of drug release as a design variable. This will be the subject of a future study. Hence in the following we have assumed a constant concentration of the drug at the needle surface.

To obtain the results efficiently the model was created in Abaqus as an input file. First, the trabecular bone geometry used in the previous study was reconstructed [6]. The following parameters were used for the geometry and it was meshed using a fluid element in Abaqus (i.e. FC3D8 fluid element): Needle diameter of 0.75 mm, bone cylinder diameter of 10 mm, bone height 5 mm. The mesh consisted of 4648 HEX8 elements and 9628 nodes. A 3D model was developed to simulate the 2D projection of the cylinder (Figure 1). In order to maintain the 2D boundary conditions, the fluid velocities on both sides out of the plane were set to be zero (i.e., symmetry condition). The top and bottom part of the model in Figure 1 was assumed to be the wall and there was only one inlet and outlet in the model. The inlet velocity (or pressure) was prescribed. This study uses the velocity boundary conditions for the inlet. The pore pressure at the outlet was set to be zero. For the bone sample, we assigned a porosity, effective diffusion coefficient, and permeability (see Eqn. 7 and 14). While Abaqus allows to use the Carman-Kozeny equation which relates the permeability to porosity, we have assigned this parameters independently in the current study [4].

At the centre of the trabecular bone sample at the needle surface, a source of drug with a constant value (2 mg/cm^3) as a boundary condition was applied. We used 2 hours as the simulation time. However, we have run simulations for 5 days which essentially showed no relative differences (results not shown in this paper). We observed that the short time scale of 2 hours is sufficient to reach steady-state phase for the chosen parameters in some cases in current study (Figure 3). The main objective of this study was to investigate the effect of the trabecular bone sample characterised by porosity, effective diffusivity, hydraulic permeability, and perfusion rate on spatial and temporal distribution of drug in the bone sample.

In fluid mechanics and transport of mass, the flow is categorized based on dimensionless quantities. Reynolds number ($Re = VL/\mu$) demonstrates relative viscous and inertial flows, where V is the characteristic velocity, L is a representative length scale and μ is fluid's kinematic viscosity. Also, Peclet number ($Pe = VL/D_{eff}$) describes the relative effect of advection and diffusion. For instance, $Pe << 1$ indicates that diffusion is dominant and vice versa. Pe number will be used to compare different simulations.

A separate python file was written to perform postprocessing of the numerical results. This file consisted of the definition of certain nodes to obtain a plot of the concentration versus time at these nodes (see dashed line in Figure 1 right). A MATLAB R2013a (8.1.0.604) function was used to solve the python file and the input files simultaneously for a parametric study in this investigation. The parameters used in this study are listed in Table 2.

Parametric studies were conducted on porosity, effective diffusivity, hydraulic permeability, initial inlet velocity to better understand the role of these factors on spatial and temporal drug concentration within trabecular bone.

3 RESULTS

Figure 2 shows the contour plots of the concentration of drug for different time points (i.e.,

columns) for three cases of bioreactor perfusion rates. Figure 2A and B show a fast perfusion rate and no perfusion rate (i.e. diffusion only case), while Figure 2C shows an average perfusion rate.

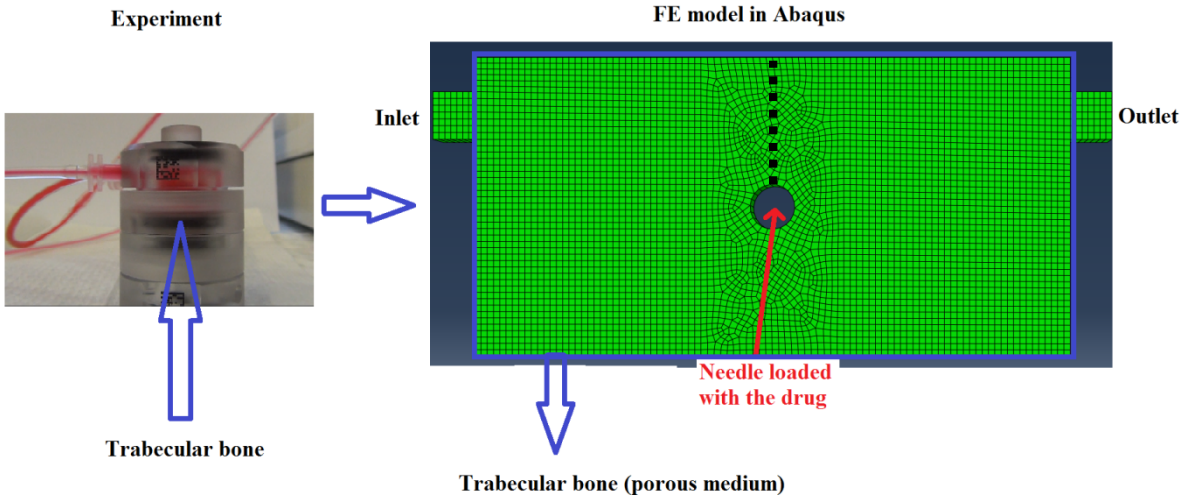

Figure 1: The geometry of the model developed in Abaqus as projection of the 3D cylinder of bone sample in the experiment explained in previous study [6]. The results will be presented as contour plots and concentration along the dashed line above the needle (see Figures 3, 4 for contour plots).

Table 2: Parameters used in this study. Each simulation used a set of variables for permeability (K), inlet velocity (V), effective diffusivity, fluid viscosity, and porosity.

Simulation	K	V	D_{eff}	ρ_f	C_{fp}	Cs	ρ_s	C_{sp}	ϵ	μ
Z100	1e-9	3e-4	1e-9	1000	1e-3	0	2300	0	0.7	4e-7
Z101	1e-9	0	1e-9	1000	1e-3	0	2300	0	0.7	4e-7
Z200	1e-10	3e-4	1e-9	1000	1e-3	0	2300	0	0.7	4e-7
Z201	1e-10	0	1e-9	1000	1e-3	0	2300	0	0.7	4e-7
Z300	1e-8	3e-4	1e-9	1000	1e-3	0	2300	0	0.7	4e-7
Z301	1e-8	0	1e-9	1000	1e-3	0	2300	0	0.7	4e-7
Z400	1e-10	3e-4	1e-10	1000	1e-3	0	2300	0	0.7	4e-7
Z401	1e-10	0	1e-10	1000	1e-3	0	2300	0	0.7	4e-7
Z500	1e-8	3e-4	1e-8	1000	1e-3	0	2300	0	0.7	4e-7
Z501	1e-8	0	1e-8	1000	1e-3	0	2300	0	0.7	4e-7
Z600	1e-8	1e-4	1e-8	1000	1e-3	0	2300	0	0.7	4e-7
Z601	1e-8	0	1e-8	1000	1e-3	0	2300	0	0.7	4e-7
Z700	1e-9	3e-4	1e-9	1000	1e-3	0	2300	0	0.6	4e-7
Z701	1e-9	0	1e-9	1000	1e-3	0	2300	0	0.6	4e-7
Z800	1e-9	3e-4	1e-9	1000	1e-3	0	2300	0	0.9	4e-7
Z801	1e-9	0	1e-9	1000	1e-3	0	2300	0	0.9	4e-7

Cleary in Figure 2A, we observe that the drug is being transported in a narrow region towards the outlet of the bioreactor. This indicates that the advective driving force is large compared to the diffusive driving force contributing to drug transport in the bone sample which is expressed as large Peclet number, i.e., Pe >>1. Figure 2B shows the static case i.e. diffusion only with zero fluid. Finally, Figure 2C demonstrated that advection is still dominant since the majority of drug is released near the outlet. We expect that the latter case is what could happen in the actual experiments of the bioreactor. In terms of drug distribution, one can clearly observe that case 2B is able to distribute the drug into the entire bone region. On the other hand, even for the case of moderately perfusion in a bioreactor (Figure 2C), there is a tendency for the drug to be distributed in the downstream regions of the bone sample while the upstream region has zero drug concentration.

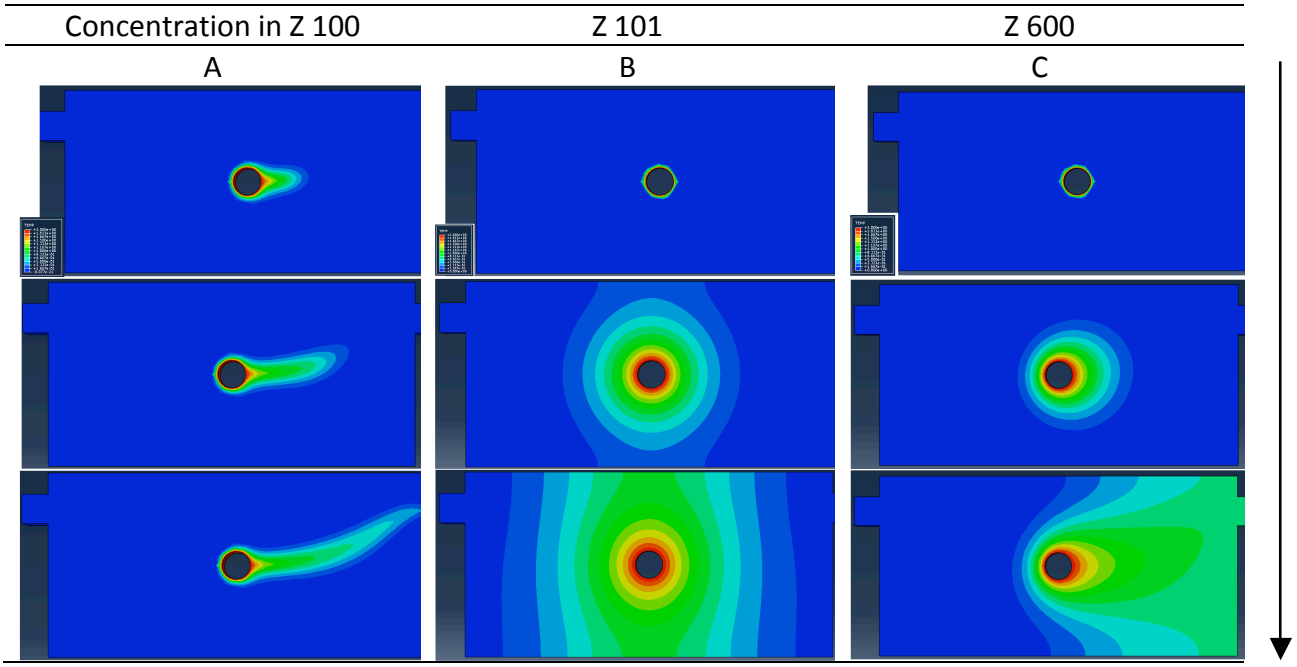

Figure 2: Contour plots of drug concentration in the trabecular bone sample at discrete time points (vertical arrow on the right hand indicates discrete time points): A) high perfusion rate (Z100), B) no perfusion (static case), i.e., diffusion only (Z101), and C) moderate perfusion (Z 600) (time points, i.e., columns: initial t=~0 sec; final t=7200 sec in bottom row, and the second row is a time point between 0 and 7200 sec)

Perfusion velocity did not significantly change following changes in permeability (Figure. 3). While permeability was varied from 1e-10 to 1e-8 [m2] the perfusion rate tended to reach the same velocity above the needle loaded with the drug.

It turned out that effective diffusivity has the most significant impact on drug distribution in the bone sample. Figure 3 shows that increased effective diffusivity could change drug distribution from transient to steady state (compare Z 300 to Z 501). For effective diffusion coefficient of $1.0e^{-10}$ or Z501, the simulation for the static case (diffusion only) showed that steady state was reached in 2 hours, but for the two other cases (Z301 and Z401) steady state was not reached. For the coupled advection-diffusion problem, the large coefficient diffusion

in Z500 strongly affects the concentration profile. This is an indication that Pe number has been reduced compared to the two other perfusion simulations i.e. Z300, and Z400. While these two latter cases had no influence on the drug distribution for perfusion flow but perfusion flow in Z500 led to a significant change in the concentration profile.

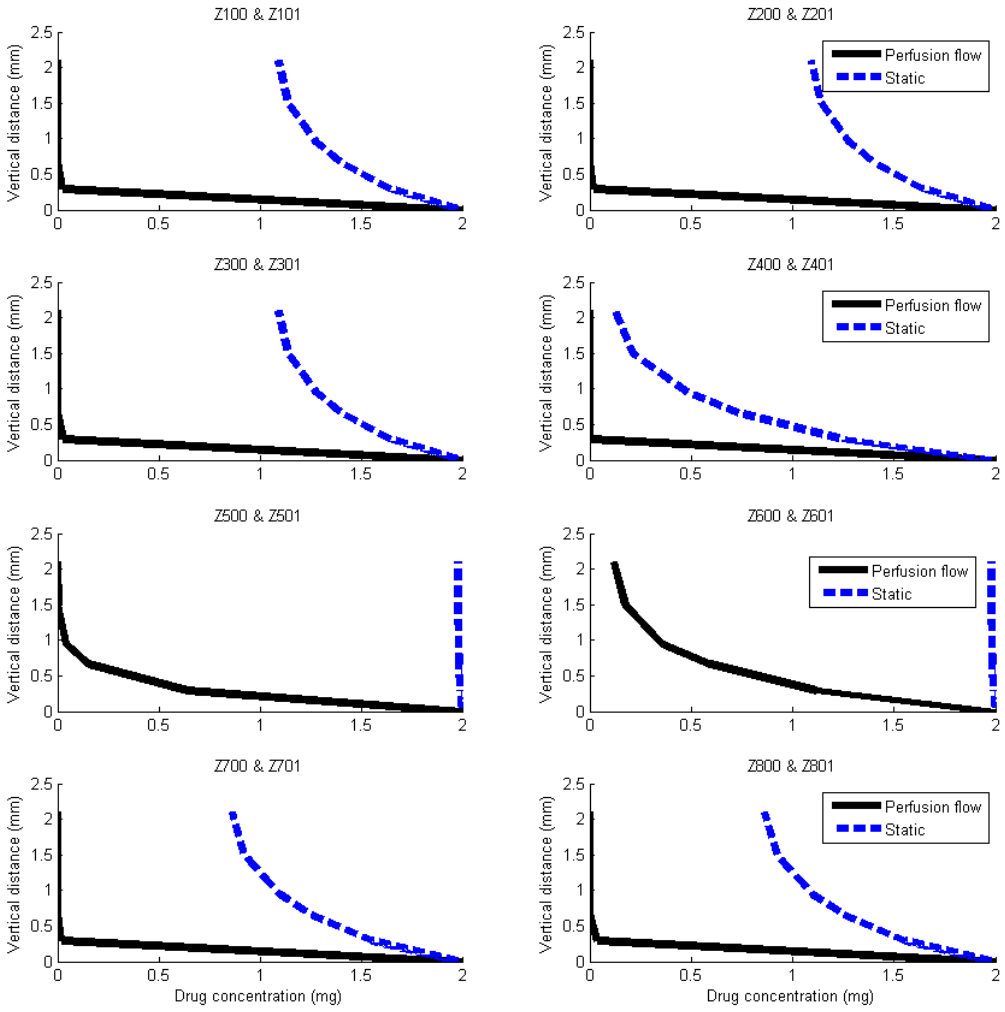

Figure 3: Concentration versus distance from needle surface plots at the last time point (t=7200 sec or 2 hours): Z100 to Z 801 from left to right (see Table 2). Each plot shows static (i.e., diffusion only) and perfusion case.

Although perfusion was almost constant due to changes in permeability, the changes in inlet velocity (or perfusion rate) resulted in significant differences in drug distribution and the shape of steady state. Figures 2 and 3 show that increased inlet velocity could wash away almost all the drug that is being released from the needle from the centre of trabecular bone. In addition, Figure 4 shows the significant effect of perfusion rate on the velocity

profile in horizontal direction for Z500 and Z600.

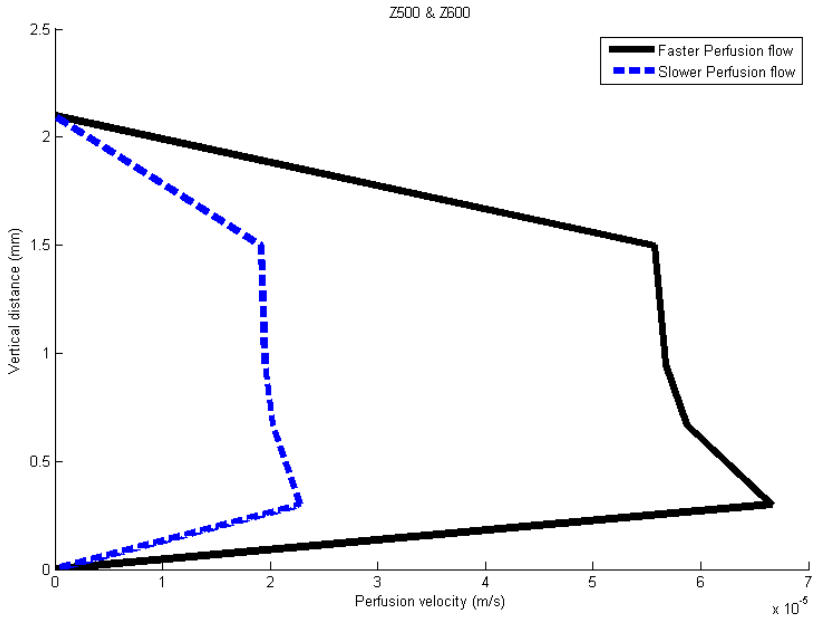

Figure 4: horizontal velocity above the needle for two different perfusion rate (Z500 vs. Z600). This figure clearly shows the effect of flow rate on velocity profile that changes Pe number and the spatial and temporal drug concentration above the needle.

4 DISCUSSION

We investigated the effect of drug transport through a trabecular bone sample bioreactor characterised by porosity, effective diffusivity, hydraulic permeability, and perfusion rate on spatial and temporal distribution of drug in the bone sample using the FE method. The current model takes advantage of fully coupled fluid flow in a porous media to solve diffusion or advection/diffusion problem in the bone sample. The heat transfer analogy was used to model the diffusion problem. Our results showed that for the permeability range investigated no major changes in drug transport were observed. On the other hand, the effective diffusivity and perfusion rate has a significant effect on the spatio-temporal distribution of the drug.

Changes in trabecular bone porosity also had minimal effect on the drug profile. In general, the permeability and porosity of a porous material are related. However, for the present study we investigated these variables separately. This could be a limitation of the present study.

Permeability in cancellous bone of bovine was found to be anisotropic [7]. However, we assume that major perfusion occurs in 2D direction and the effect of perfusion in the direction perpendicular to the inlet and outlet is negligible. As a result, it is acceptable to consider the isotropic permeability in our simulations. In addition, to predict the role of permeability on fluid flow around the needle and on the drug release kinetics, we increased the permeability from 1e-10 m^2 to 1e-8 m^2. The results suggest that permeability may not play a major role in drug concentration profile. On the other hand, Darcy law suggest that an increase in permeability will directly increase flow rates, thereby, increasing the fluid velocity. The

reason for this discrepancy may be other non-Darcian terms in Eqn. 6 that influence velocity profile in the bone sample. Finally, it has also been shown that permeability is related to the Reynolds number which has to be considered in future studies [8].

Effective diffusivity was found one of the major variables that influenced the diffusion only case and perfusion flow in the current study. Figure 3 (Z301 and Z501) shows that the increase in effective diffusivity could enhance the spatial distribution of the drug. In particular, Z501 simulation reached steady state in 2 hours while perfusion flow also increased drug concentration above the needle (Z500). This means that to design an optimized local drug delivery system in a bioreactor one needs to carefully consider the effect of fluid flow and diffusion properties of the drug. The drug diffusion also depends on microstructure of the bone matrix that would change porosity within a bone sample; however, current study has considered the same porosity across the trabecular bone sample. The effect of different porosity within a bone sample as well as changes in effective diffusion due to microstructure variations may reveal other aspects of combined role of pore size, pore size distribution and variation in effective diffusivity on drug release kinetics in future studies [9,10].

Finally, it was found that perfusion rate plays a major role on drug distribution even for the short 2 hours simulation time. However, it should be noted that the influence of perfusion rate changes Pe number in which effective diffusivity plays a major role. In order to address the role of these two variables in a more realistic simulation, accurate values from experiments and the natural variability among these variables are required. The information about these variables enables us to predict the optimal range for drug distribution which is the subject of a future investigation. In addition to the variables considered in this study, the role of needle size and needle's placement angle in bone, bone sample size, mechanical loading should also be considered in future studies.

This study involves a number of limitations. We developed a semi 3D model of trabecular bone sample as a slice of constant thickness of the 3D bone sample in the bioreactor. We did not aim to validate our results with the 3D experimental results obtained previously. This was due to the fact that we aimed to compare the role of different design variables on the spatio-temporal concentration profile in the bone sample; therefore, a thorough validation of the model with experiments is required. It is also impractical to measure accurate inputs to the model such as pore pressure, inlet velocity, and other structural and fluid's variables. Therefore, a comparative study was conducted to visualize the differences quantitatively. Another study is required to investigate the sensitive analyses of these variables on our findings. In current study, our simulations showed the results up to 2 hours. This can easily be extended to a larger time scale and can be compared with experimental studies using bioreactors with the aid of sufficient computational power.

5 CONCLUSIONS

The study of parameters characterizing the trabecular bone sample (porosity, effective diffusivity and permeability) and the perfusion rate of the bioreactor suggest that local drug delivery is a multifactorial problem. To design a proper drug delivery system for a porous material such as bone one has to take into account the combined effects of these variables to enhance the uniform distribution of drug across the bone sample. The current study clearly shows that computational modelling can be used as an *in-silico* tool to investigate the large

number of design variables. Once significant factors characterizing the problem have been identified targeted experiments can be performed.

ACKNOWLEDGEMENT

Dr Pivonka, Dr Atkins, Dr Findlay and Dr Losic gratefully acknowledge financial support of this project by the Australian Research Council (DP120101680).

REFERENCE

[1] Kim M, Gillies R, Rejniak K. Current advances in mathematical modeling of anti-cancer drug penetration into tumor tissues. *Front Oncol*. (2013).

[2] Hose DR, Narracott a J, Griffiths B, et al. A thermal analogy for modelling drug elution from cardiovascular stents. *Comput Methods Biomech Biomed Engin*. (2004)**7**(5):257–64.

[3] Siepmann J, Peppas N a. Modeling of drug release from delivery systems based on hydroxypropyl methylcellulose (HPMC). *Adv Drug Deliv Rev*. (2001) **48**(2-3):139–57.

[4] Nield DA, Bejan A. Convection in porous media. *Springer*; 2006.

[5] Abaqus. Documentation, A. B. A. Q. U. S. "*Version 6.6, ABAQUS*." (2013).

[6] Aw MS, Khalid K a, Gulati K, et al. Characterization of drug-release kinetics in trabecular bone from titania nanotube implants. *Int J Nanomedicine*. (2012) **7**:4883–92.

[7] Kohles SS, Roberts JB, Upton ML, Wilson CG, Bonassar LJ, Schlichting a L. Direct perfusion measurements of cancellous bone anisotropic permeability. *J Biomech*. (2001) **34**(9):1197–202.

[8] Edwards D, Shapiro M. The influence of Reynolds number upon the apparent permeability of spatially periodic arrays of cylinders. *Phys Fluids A* (1990).

[9] Spencer TJ, Hidalgo-Bastida L a, Cartmell SH, Halliday I, Care CM. In silico multi-scale model of transport and dynamic seeding in a bone tissue engineering perfusion bioreactor. *Biotechnol Bioeng.* (2013) **110**(4):1221–30.

[10] Cardoso L, Fritton SP, Gailani G, Benalla M, Cowin SC. Advances in assessment of bone porosity, permeability and interstitial fluid flow. *J Biomech*. (2013) **46**(2):253–65.